ALGORITHMS OF SPACE VECTOR PWM IN OVERMODULATION AREA

Z. Peroutka, T. Glasberger

University of West Bohemia / Department of Electromechanics and Power Electronics, Plzeň, Czech Republic
e-mail:peroutka@ieee.org, tglasber@kev.zcu.cz

Summary The aim of this paper is the comparison and evaluation of different space vector PWM (SVPWM) strategies enabling the continuous transition from the linear modulation to the six-step mode. One of the important factors to be explored is the frequency analysis of the motor quantities in order to be able to evaluate the possible impact of the drive on the traction mains – specifically the impact on the railway signaling.

This research has been supported by the Ministry of Industry and Trade of the Czech Republic under the project MPO ČR FI-IM2/071.

1. INTRODUCTION

Space vector PWM (SVPWM) is eligible for the modern control algorithms of adjustable speed drives and active rectifiers. The operation of this modulation scheme in the overmodulation area as well as continuous transition into the six-step mode is still under the research (e.g. [1] – [3]). The operation in the overmodulation area and the transition into the six-step mode can cause the problems not only from the control viewpoint, but can also be the source of the serious problems in the traction applications – e.g. adverse interaction of the traction drive with the railway signaling, what is one of our important research objective.

2. SVPWM IN OVEMODULATION AREA

A. Overmodulation Strategy 1 (OS1)

This algorithm [2] is quite simple for the implementation. The principle of the overmodulation algorithm 1 is illustrated in the Fig. 1.

The demanded voltage vector u* (control command) is produced so long, until its circular trajectory intersects the hexagon edge (Fig. 1a, in this mode $u^* = u_{sk}$, where u_{sk} is the real converter output voltage vector).

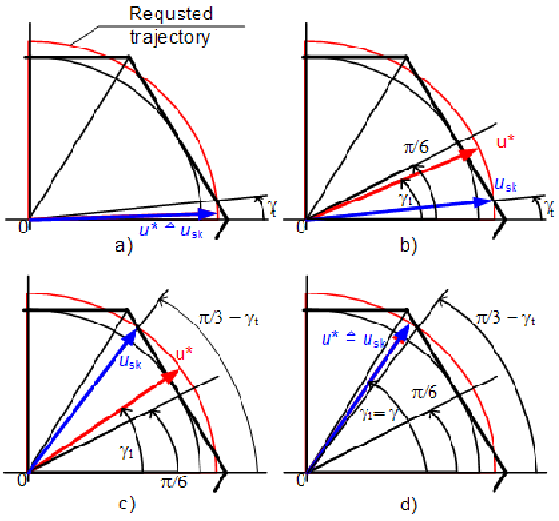

Fig. 1. Principle of the first investigated overmodulation algorithm (OS1): (γ… position of the real converter output voltage vector $\boldsymbol{u}_{sk}$, γ_t … position of demanded voltage vector $\boldsymbol{u}^*$, γ_t… hold angle)

When the vector u* intersects the hexagon edge (Fig. 1b), the real converter output vector u_{sk} stays in this constant position (γ_t – so called hold angle), while the demanded vector u* moves to ($\pi/6$) in the given sector. Thereafter the real vector jumps to the position ($\pi/3 - \gamma_t$), (Fig. 1c). When the vector u* achieves position ($\pi/3 - \gamma_t$) – it means that u* intersects the hexagon edge again, then the converter produces the real vector u_{sk}, which corresponds with demanded vector u* ($u_{sk} = u^*$) – symmetric action in the hexagon vertexes (Fig. 1d).

B. Overmodulation Strategy 2 (OS2)

This overmodulation strategy is based on [3]. In this method, the overmodulation area is divided using the modulation index mi_1 (1) into two sub-areas: overmodulation area I and II (OAI and OAII respectively). The modulation index is defined as:

$$mi_1 = \frac{|u^*|}{U_{max}}, \qquad (1)$$

where $|u^*|$ is size of the demanded voltage vector, $U_{max} = (2/3U_{dc})$ is maximum phase voltage accessible in the six-step mode and U_{dc} is the converter dc-link voltage. Thus, the index mi_1 shows the actual utilization of the converter voltage capability.

In the overmodulation area I, the reference vector size is changed, while the reference voltage vector angle is maintained – the demanded voltage vector angle and real converter output voltage vector angle

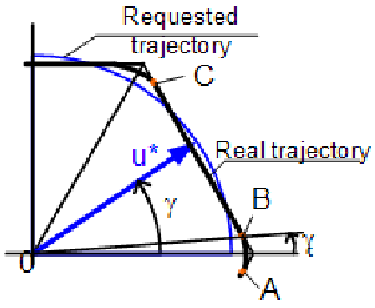

Fig. 2. OS2: Space vector trajectory in overmodulation area I

is the same. If the demanded voltage vector u* is inside the hexagon (between points A-B), the

modulation employs common strategy for linear modulation area [4].

When the demanded vector u* trajectory passes outside the hexagon (the demanded voltage vector is out of the converter voltage capability), the switching times must be calculated with (2), the zero vector is not used and the real converter output voltage vector u_{sk} moves along the hexagon edge, that is between points B-C as is shown in the Fig. 2.

$$T_1 = \frac{T_{pwm}}{3} . \frac{\alpha}{\pi/3}, \qquad (2a)$$

$$T_2 = T_{pwm} - T_1, \qquad (2b)$$

where T_1 is the switch on time of the first outer vector, T_2 is the switch on time of the second outer vector and T_{pwm} is PWM period.

$$\gamma_{sk} = 0 \quad \text{for} \quad 0 \le \gamma \le \gamma_t, \qquad (3a)$$

$$\gamma_{sk} = \frac{\gamma - \gamma_t}{\pi/6 - \gamma_t} \frac{\pi}{6} \text{ for } \gamma_t \le \gamma \le \pi/3 - \gamma_t, \qquad (3b)$$

$$\gamma_{sk} = \pi/3 \quad \text{for} \quad \pi/3 - \gamma_t \le \gamma \le \pi/3, \qquad (3c)$$

In the overmodulation area II, the real converter output voltage vector u_{sk} trajectory changes gradually from hexagon to the discrete six-step trajectory.

At first in the switching period, the real converter voltage vector u_{sk} stays in the outer position, which corresponds with the six-step mode (Fig. 3a). When the demanded voltage vector u^* position reaches the hold angle γ_t, then the real converter output voltage vector u_{sk} moves along the hexagon edge (Fig. 3b). This operation is symmetrically repeated on the second side of the sector in order to produce symmetrical pulse pattern of the converter output voltage (Fig. 3c,d).

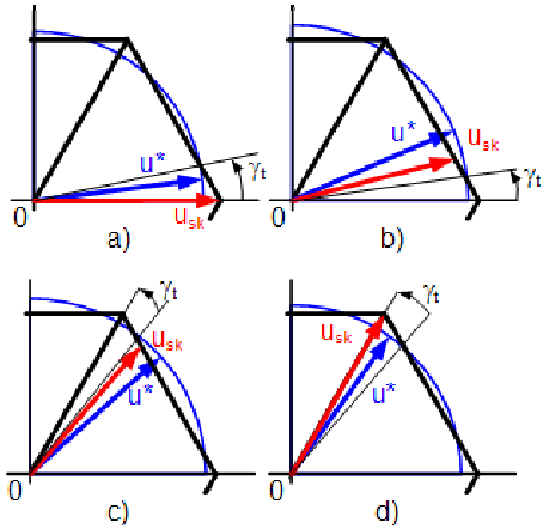

Fig. 3. OS2: Modulation strategy in the overmodulation area II: demanded (u) and real converter output voltage vector (u_{sk}) trajectory*

The position (γ_{sk}) of the converter output voltage vector u_{sk} corresponding to the given demanded vector u* is calculated by (3).

C. *Overmodulation Strategy 3 (OS3)*

This algorithm based on [1] uses the modulation depth (mi_2) in order to divide the modulation area into the linear modulation area ($mi_2 \le 1$) and two overmodulation ranges: overmodulation area I (OAI: $mi_2 \in (1, 1.05)$) and overmodulation area II (OAII: $mi_2 \in (1.05, 1,1)$). The modulation depth is given by:

$$mi_2 = \frac{2}{\sqrt{3}} . \frac{|u^*|}{U_{\max}} = \frac{\sqrt{3}|u^*|}{U_{dc}}, \qquad (4)$$

where $|u^*|$ is size of the demanded voltage vector, $U_{max} = (2/3U_{dc})$ is maximum phase voltage accessible in the six-step mode and U_{dc} is the converter dc-link voltage.

In the overmodulation area I, the reference vector moves along the circular trajectory with the radius equal to the modulation depth mi_2 near the hexagon vertex. From the specific angle γ_t, the real converter output voltage vector u_{sk} jumps on the hexagon edge and moves along this edge until it reaches the position ($\pi/3$ - γ_t). Thereafter the reference vector trajectory is again circled. This algorithm is depicted in the Fig. 4. The switching times are in the overmodulation area I calculated by (5):

$$T_1 = \frac{mi_1 . \sin(60 - \gamma)}{mi_1 . \sin\gamma + mi_1 . \sin(60 - \gamma)} . T_{pwm}, \qquad (5a)$$

$$T_2 = T_{pwm} - T_1, \qquad (5b)$$

In the overmodulation area II, the reference voltage vector size and also its phase angle are distorted. The modulation strategy in the overmodulation area II is almost the same as in the above described strategy OS2.

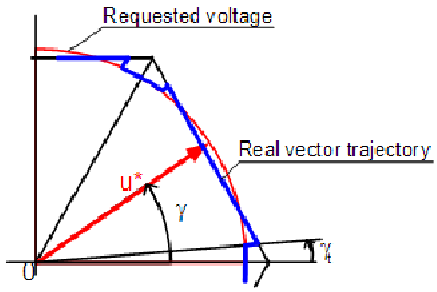

Fig. 4. OS3: Converter output voltage vector trajectory in overmodulation area I

3. COMPUTER SIMULATION

The simulation results of the first overmodulation strategy OS1 are depicted in the Fig. 5. Fig. 6 shows the motor phase voltage and motor phase current from the second method (OS2). Fig. 7 presents results from OS3, both in area OAI. Fig. 8 and Fig. 9 display results from the same method, but in OAII.

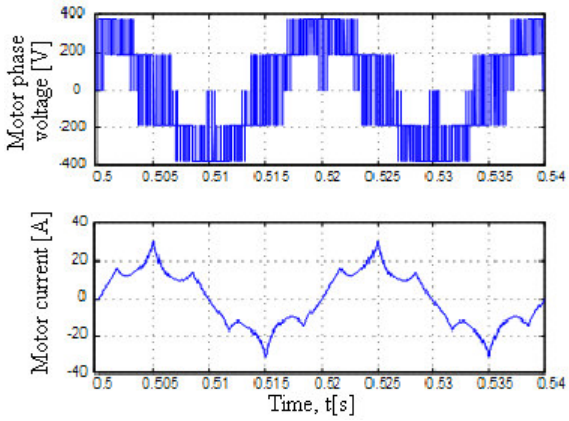

Fig. 5. Behaviour of overmodulation strategy 1 (OS1) described in 2.A: f_{pwm} = 4kHz, f_{out} = 50Hz, dc-link voltage U_{dc} = 565V, $|u^*|$ = 343V.

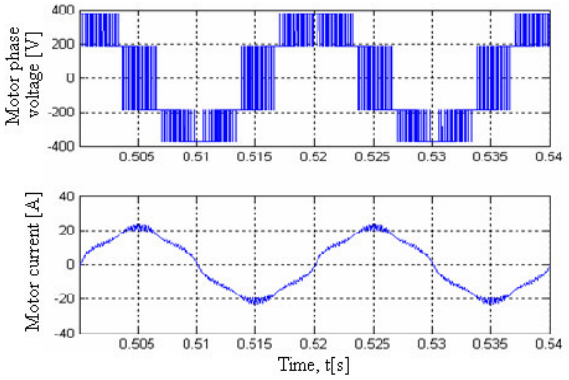

Fig. 6. Behaviour of overmodulation strategy 2 (OS2) in the overmodulation area I (see paragraph 2.B): f_{pwm} = 4kHz, f_{out} = 50Hz, dc-link voltage U_{dc} = 565V, $|u^*|$ = 336V.

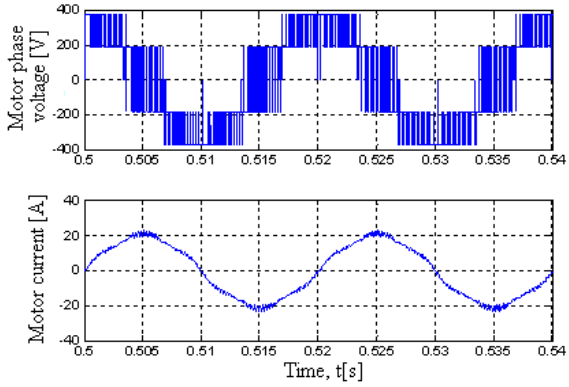

Fig. 7. Behaviour of overmodulation strategy 3 (OS3) in the overmodulation area I (see paragraph 2.C): f_{pwm} = 4kHz, f_{out} = 50Hz, dc-link voltage U_{dc} = 565V, $|u^*|$ = 336V.

4. EXPERIMENTAL EVIDENCE

The above explored algorithms (OS1 – OS3) have been implemented in the fixed-point digital signal processor Texas Instruments TMS320LF2812.

In linear modulation area, the approach published in [4] has been applied. The designed SVPWM has been tested on the induction machine drive of rated power of 4kW (IM: 4kW, 380V/50Hz, 1420rpm). The simple open loop V/f control has been selected for the tests, because it make possible to easily change the preset ramp and, therefore, to define various conditions for the experimental verification of the modulation strategies under the test.

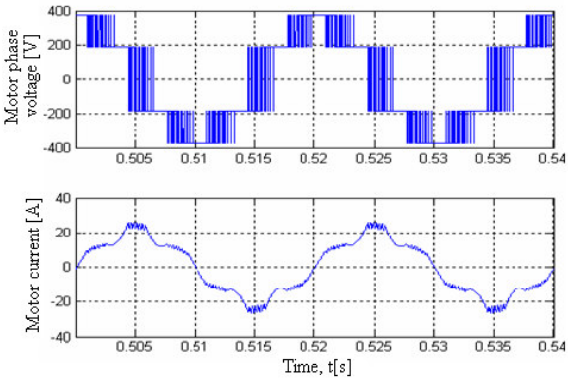

Fig. 8. Behaviour of overmodulation strategy 2 (OS2) in the overmodulation area II (see paragraph 2.B): f_{pwm} = 4kHz, f_{out} = 50Hz, dc-link voltage U_{dc} = 565V, $|u^*|$ = 346V.

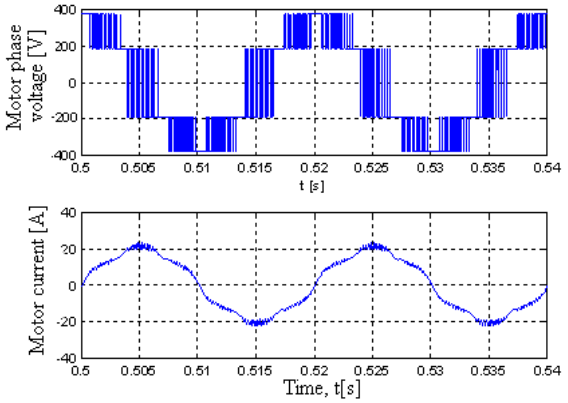

Fig. 9. Behaviour of overmodulation strategy 3 (OS3) in the overmodulation area II (see paragraph 2.C): f_{pwm} = 4kHz, f_{out} = 50Hz, dc-link voltage U_{dc} = 565V, $|u^*|$ = 346V.

Based on the simulation results, the strategy OS3 has been highlighted, because it provides in our opinion very good properties. Fig. 10 – Fig. 13 presents both the waveforms and the frequency analysis (on-line FFT) of the motor phase voltage and motor current in both overmodulation area I (f_{out} = 45Hz) and overmodulation area II (f_{out} = 48Hz) (strategy OS3). Switching frequency has been f_{pwm} = 4kHz and dc-link voltage U_{dc}=540 V. In the linear modulation area and overmodulation area I, there dominate the first harmonic component and harmonics around the multiples of the switching frequency f_{pwm} (the side bands based on the f_{out} multiples). In the overmodulation area II, where the converter output voltage is near the six-step mode, there appear the well-known harmonics: 5^{th}, 7^{th}, etc. These results are well-known. However, our attention has been paid to the low frequency harmonics (up to 100Hz) that can potentially disturb the railway signaling.

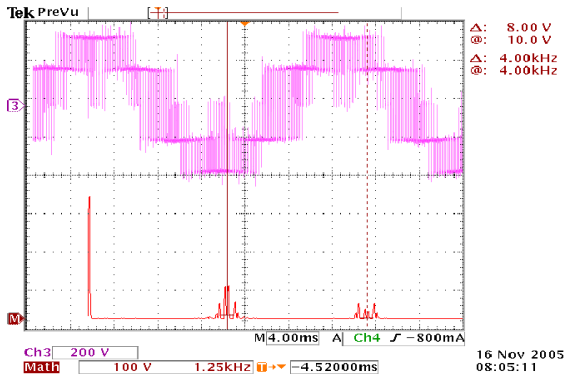

Fig. 10. Strategy OS3 – overmodulation area I: Frequency analysis (on-line FFT) of motor phase voltage

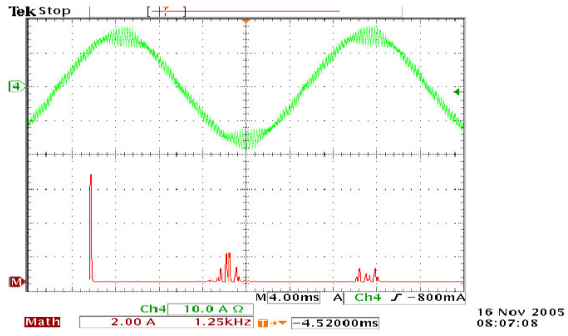

Fig. 11. Strategy OS3 – overmodulation area I: Frequency analysis (on-line FFT) of motor phase current

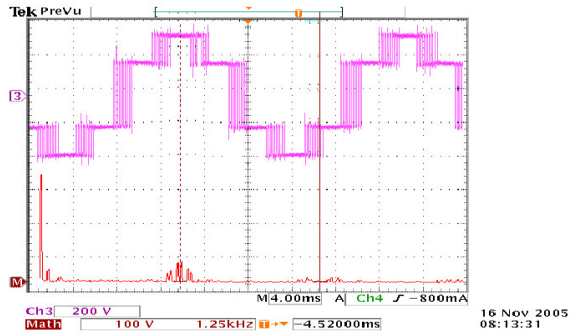

Fig. 12. Strategy OS3 – overmodulation area II: Frequency analysis (on-line FFT) of motor phase voltage

5. CONCLUSIONS

The first criterion for overmodulation algorithms comparison is the computing time. The method OS1 is quite simple; the computing time of this method is the shortest. The other two algorithms (OS2 and OS3) have almost similar principle; thus, their computing times are similar too (computing time has taken 4.5µs with DSP TI TMS320LF2812 operating at clock frequency of 75MHz).

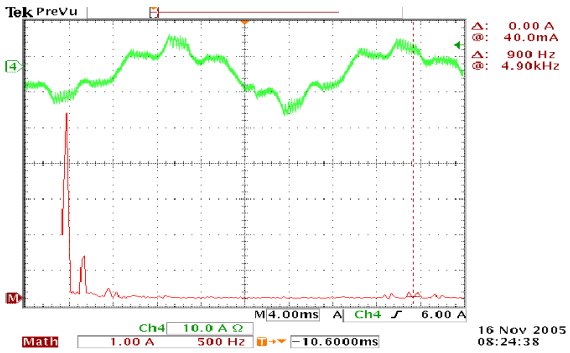

Fig. 13. Strategy OS3 – overmodulation area II: Frequency analysis (on-line FFT) of motor phase current

The next criterion is behaviour (quality) of motor quantities. From the results in the time domain and frequency analysis can be concluded that the strategy OS1 provides the worst behaviour of explored motor quantities. The motor quantities in case of the other two methods are on first sight comparable, but the current behaviour in overmodulation area II of OS2 is more distorted.

In this paper, the attention has been paid to asynchronous modulation. The frequency analysis has been focused on the low frequency components especially of the motor current (up to 100Hz) in order to be able to evaluate the possible impact of the modulation on the dc traction mains. Our observations show that danger low frequency components are mainly influenced by switching frequency (f_{pwm}). In the high power traction applications (such as locomotives) the switching frequency is limited to hundreds hertzs. Therefore, the important role plays the proper selection of the ration between f_{pwm} and the railway signalling frequency. It is important to note that all of these asynchronous SVPWM algorithms cannot provide satisfactory operation under very low switching frequencies (approx. less than 800 Hz).

REFERENCES

[1] Bakhshai R. A., Joós G., Jain P., K., Jin H.: *Incorporating the Overmodulation Range in Space Vector Pattern Generators Using a Classification Algorithm*. IEEE Transactions on Power Electronics, Vol. 15, No. 1, Jan. 2000.

[2] Bolognani S., Zigliotto M.: *Novel Digital Continuous Control of SVM Inverters in the Overmodulation Range*. IEEE Transactions of Industry Applications, vol. 33, No. 2, March/April 1997.

[3] Holtz J., Lotzkat W., Khambadkone A. M.: *On Continuous Control of PWM Inverters in the Overmodulation Range Including the Six-Step Mode*. IEEE Transactions on Power Electronics, Vol. 8, No. 4, October 1993.

[4] Peroutka Z.: *Space Vector Pulsewidth Modulation for Modern Control Algorithms*. In: Elektrotechnika a informatika 2003. ZČU v Plzni, Plzeň 2003. pp. 92-95, Vol. II. ISBN 80-7082-922-3.